Title

When hot nights will not allow to relax: Projections of co-occurring extreme heat events over Central Europe under policy-relevant global warming levels

Abstract

Co-occurring heat extremes that combine warm days with warm nights can generate sustained heat stress and reduce nighttime recovery, increasing risks to health and socio-economic systems. We assess how such day–night heat co-occurrences are projected to evolve over Central Europe using the Global Warming Level (GWL) framework. To strengthen decision relevance, we evaluate not only Paris Agreement-aligned thresholds (1.5 °C and 2.0 °C) but also policy-relevant warming levels consistent with outcomes under national pledges and current policies (1.9 °C and 2.7 °C). Projections are derived from two performance-informed sub-ensembles of CMIP6 climate simulations and are analysed spatially and for selected NUTS administrative regions, aligning results with governance and adaptation planning needs. NUTS-level outputs for six Central European countries are provided via an open Zenodo repository.

Co-occurrence events were rare during the observational period (1995–2014) over most of the domain, with localized hotspots in warmer lowland areas, particularly in Hungary. At the studied GWLs, the affected area is wider, and co-occurrence frequencies rise strongly, with a marked emergence and intensification of hotspots between 1.9 °C and 2.0 °C. Hungary and Slovakia consistently show the highest projected frequencies and the longest persistent events, indicating elevated heat risk. Uncertainty is dominated by differences between models; scenario effects are generally smaller but increase at higher warming levels. Overall, relatively small increments in global warming can produce disproportionate increases in the frequency and persistence of co-occurring day–night heat extremes, underscoring the value of region-specific adaptation planning under policy-consistent warming futures.

Practical implications

Heat extremes are among the most consequential climate hazards in Central Europe, affecting public health, labour productivity, infrastructure performance, and energy systems. Risks are particularly elevated when hot days co-occur with warm nights that prevent physiological recovery, thereby increasing cumulative heat stress and placing sustained pressure on vulnerable populations and critical services. Planning based solely on daytime heat indicators may therefore underestimate the overall burden of heat-related impacts. At the same time, there is a growing divergence between internationally agreed climate targets and the warming levels implied by currently implemented policies. While the Paris Agreement aims to limit global warming to 1.5 °C and well below 2.0 °C, current policy trajectories are more consistent with higher warming outcomes. Adaptation planning may therefore benefit from considering not only normative targets but also policy-consistent warming levels that are plausible under present mitigation efforts.

This study contributes to this need by assessing the frequency and persistence of co-occurring day- and night-time heat extremes at four Global Warming Levels (1.5 °C, 1.9 °C, 2.0 °C and 2.7 °C above pre-industrial levels). The inclusion of 1.9 °C and 2.7 °C reflects warming levels associated with current pledges and policies, thereby aiming to strengthen the relevance of the projections for decision-making contexts. Results are aggregated to NUTS administrative regions across six Central European countries, aligning climate information with governance structures responsible for regional adaptation planning and EU funding implementation. The analysis provides two key indicators: annual frequency of co-occurring events and maximum duration of consecutive events within each warming level.

The projections suggest that relatively small increments in global warming may be associated with disproportionate increases in both frequency and persistence of co-occurring heat events. Several regions, particularly in Hungary and Slovakia, appear more strongly affected under higher warming levels. These findings may support the consideration of nighttime heat thresholds and persistence metrics in heat-health warning systems, regional risk assessments, and infrastructure planning. For example, regional authorities could compare projected event duration under 1.5 °C and 2.7 °C warming to assess whether existing heat-health action plans remain sufficient under policy-consistent warming conditions.

By expressing impacts relative to global temperature thresholds, the framework seeks to facilitate adaptation planning under uncertainty and to clarify potential regional differences across mitigation outcomes. Results for the NUTS regions are provided in an open repository in commonly used formats, enabling their practical application in decision making processes. In this way, the study aims to contribute decision-relevant information that can be directly integrated into regional climate services and adaptation strategies in Central Europe.

1. Introduction

Humanity is already experiencing the impacts of global warming, which are projected to intensify even if current mitigation efforts are fully achieved (IPCC, 2023; WMO, 2025; Ripple et al., 2025). Among these impacts, heat-related extremes are particularly concerning due to their potential to negatively affect human health, ecosystems, and infrastructure, as well as labour and economic activity, and broader socio-economic systems (Matthews et al., 2017; Denissen et al., 2024; Forzieri et al., 2017; Gasparrini et al., 2017; Gallo et al., 2024; Szewczyk et al., 2021). Days with high maximum temperatures can have a significant impact, especially when paired with elevated nighttime temperatures, creating persistent heat stress that can prevent physiological recovery and pose serious health risks to vulnerable populations, including older people, children, and those with pre-existing conditions (He et al., 2022; Liu et al., 2025).

As global warming intensifies, understanding the frequency, persistence, and spatial distribution of such co-occurring heat events is crucial for developing targeted adaptation strategies, early-warning systems, and risk-informed planning (Seneviratne et al. 2021). This requires climate information that is both credible and decision-ready. Yet the diversity of climate models, emissions scenarios, and temporal windows often obscures which specific risks policymakers and planners should anticipate. According to the latest United Nations Environmental Programme (UNEP) Emissions Gap Report (UNEP, 2025a), current national policies and pledges are insufficient to meet the Paris Agreement goals of limiting warming to well below 2 °C and preferably to 1.5 °C relative to the preindustrial baseline. Simultaneously, the UNEP Adaptation Gap Report (UNEP, 2025b) highlights the immense financial requirements for adaptation, estimating hundreds of billions of euros to meet adaptation needs. This context underscores a critical challenge: decision-makers must navigate a highly uncertain future while determining the magnitude of impacts the different regions should prepare for.

In this study, we apply the Global Warming Level (GWL) framework (James et al., 2017) to investigate how heat-related extremes develop across a range of possible global temperature increases. The GWL method links regional climate changes to a specific increase in global mean temperature compared to a predefined baseline, allowing for a consistent comparison of climate impacts across different global warming levels. A key benefit of this approach is that it enables direct alignment with the temperature goals of the Paris Agreement (King and Karoly, 2017), thereby facilitating effective communication between scientific assessments and policy targets. Studies applying the GWL method are mainly focusing on these goals or other, evenly distributed thresholds (Vautard et al, 2014; King and Karoly, 2017; Dosio et al., 2018; Kjellström et al, 2018; Jacob et al, 2018; Guo et al, 2020; Ruosteenoja and Jylha, 2023a; Ruosteenoja and Jylha, 2023b; Becsi and Formayer, 2024). However, current national policies still do not align with the Paris Agreement's goal, with most emission pathways indicating at least a slight overshoot of the 1.5°C or even the 2.0°C limit (Schleussner et al., 2016). With the GWL method it is possible to study projections of regional climate futures under different global mitigation outcomes (e.g., Climate Action Tracker (CAT, 2024). Using this framework provides a scientifically based and policy-relevant way to evaluate future heat risks. It also helps identify adaptation strategies that are both cost-effective and resilient across the most probable warming scenarios. Additionally, it may help to emphasize the benefits of stronger mitigation by showing how differences in global warming levels can affect how often and how severely heat-related hazards occur.

Beyond establishing a direct link between climate impacts and policy ambition, the GWL framework is valuable for addressing uncertainty in climate model projections

(Wartenburger et al., 2017; Seneviratne et al., 2021; Evin et al., 2024). By aligning climate model outputs according to global temperature thresholds rather than fixed time periods, the GWL approach enables consistent comparisons across models, reducing the influence of differing climate sensitivities and transient warming rates, which has been particularly important with the last generation of CMIP6 models (Sherwood et al., 2020; Zelinka et al., 2020; Hausfather et al., 2022). This alignment also diminishes the importance of socio-economic scenario choice, as many temperature-related responses are largely independent of the pathway taken, although minor scenario-dependent variations have been reported, particularly at middle and high latitudes (Wartenburger et al., 2017; Diez-Sierra et al., 2023; Evin et al., 2024). As a result, GWLs facilitate a consistent assessment of climate change impacts and help to disentangle uncertainty associated with regional climate responses—such as temperature extremes—from uncertainty related to differences in global mean warming across models (Seneviratne et al., 2016; James et al., 2017; Seneviratne & Hauser, 2020).

In this paper, we apply the GWL framework to analyse the co-occurrence of heat-related extreme events—namely summer days, hot days, and extremely hot days occurring together with tropical nights—over a Central European domain at different levels of global warming. To fully exploit the policy relevance of the GWLs, besides studying the thresholds in accordance with the Paris Agreement, we select global warming levels that correspond to temperature outcomes implied by currently implemented policies and stated national commitments to try to strengthen the connection between projected impacts and real-world policy choices (CAT, 2024). To further enhance the relevance of the results for governance and adaptation planning, we demonstrate how model outputs can be aggregated to Nomenclature of Territorial Units for Statistics (NUTS) administrative regions, i.e. standardized territorial units used in the European Union for regional statistics and policy implementation. Presenting results at these administrative levels facilitates their direct use by regional authorities and climate service providers. While in the study we analyse only selected NUTS regions in detail, we provide results for six Central European countries in an open Zenodo repository (see details in Section 2).

The development of climate change scenarios of any kind always requires the employment of more than one climate model because of unequivocal model uncertainty (Abramowitz et al., 2019). A natural choice for model selection is to pick models that show good skill in simulating present-day or historical climatic conditions, even though the good performance cannot be considered as a guarantee of reliable projections (Knutti, 2008; Reifen and Toumi, 2009; Merrifield et al., 2023;). Here, we employ two subsets of CMIP6 simulations identified in the literature as performing robustly over Europe to ensure credible regional projections. Comparison of the two subsets provides an insight into the uncertainty connected with the choice of models. One of the subset selections is based on rather large-scale performance criteria (Palmer et al., 2023), while the other is based on more regional-scale performance.

This second subset (Climrisk, see the methods below) has been created as a basis for adaptation strategies within the Czech Republic (https://urbanadapt.cz/cs).

Our analysis focuses on the temporal clustering and persistence of co-occurring heat events as well as their potential amplification with additional warming. The resulting projections provide a foundation for targeted adaptation strategies in Central Europe and can also serve as critical input for risk assessments.

2. Data and methodology

We analysed data for six Central European countries: Germany, Czechia, Poland, Austria, Hungary, Slovakia, and additionally aggregated for the NUTS regions. The NUTS framework provides a standardized hierarchical division used across the European Union for regional statistics, socioeconomic assessments, policy implementation, including climate adaptation planning (Eurostat, 2024). However, local administrative regions do not correspond to the same NUTS level across countries. To address this discrepancy, we selected for each country the NUTS level that best reflects the primary sub-national administrative scale in each country: NUTS 1 for Germany, NUTS 2 for Austria and Poland, and NUTS 3 for Czechia, Slovakia, and Hungary. Data and figures for all NUTS regions are provided in a Zenodo archive (Szabó et al., 2026).

In the following text, we provide a detailed analysis of a Central European domain extending from 47° to 53° N and 8° to 22° E (Fig. 1), used previously by Lhotka et al. (2018) and in this region we focus on selected NUTS regions: non-capital areas with relatively low socioeconomic indicators (https://ec.europa.eu/eurostat) and regions prone to climate hazards according to our results (see regions in Fig. 3-4 and Fig. S1-S4).

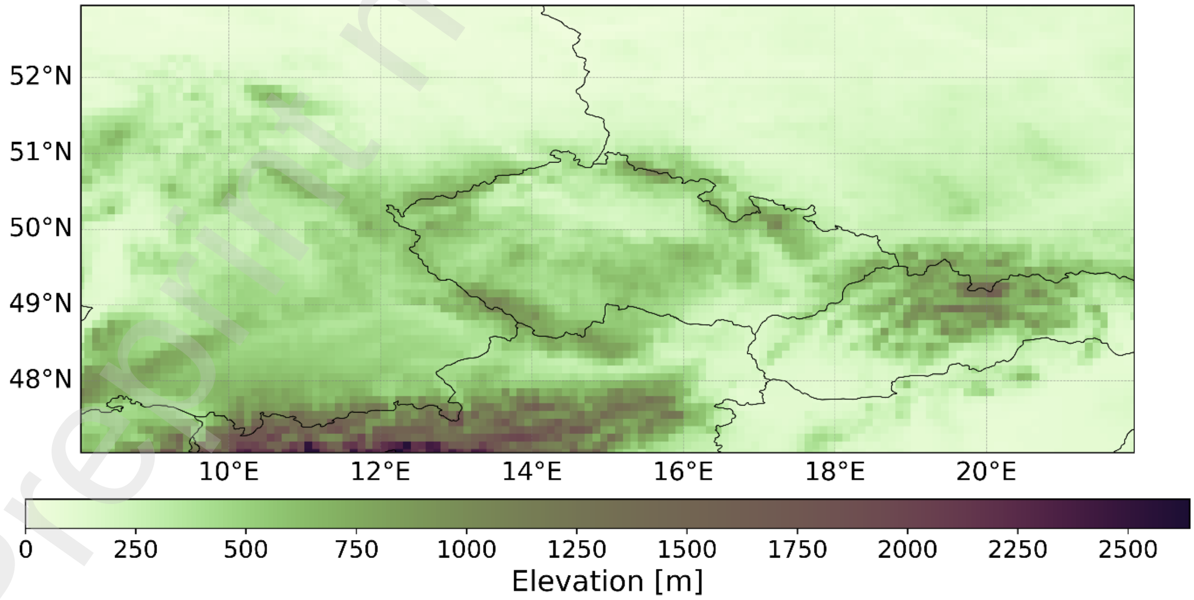

Fig. 1 Elevation over the study domain using data from E-OBS version v30.0e (Cornes et al., 2018).

2.1. *Global warming levels calculation*

For our analyses, we selected four Global Warming Levels (GWLs): 1.5 °C, 1.9 °C, 2.0 °C, and 2.7 °C. The 1.5 °C and 2.0 °C levels correspond to the Paris Agreement temperature targets, representing internationally agreed thresholds for limiting global warming. The 1.9 °C and 2.7 °C levels are based on the Climate Action Tracker (CAT, 2024) as median end-of-century warming estimates under full implementation of national pledges (1.9 °C) and current policies (2.7 °C) at the time of preparation of the study (note that in the latest CAT (2025) report, the higher end is reduced to 2.6 °C). Including these policy-consistent warming levels provides context on likely outcomes under existing mitigation trajectories.

To ensure consistency in terminology, we adopted the naming conventions of Becsi and Formayer (2024), denoting each warming level as GWL followed by the corresponding temperature anomaly relative to pre-industrial conditions (e.g., GWL1.5 represents a global mean temperature increase of 1.5 °C). Time periods corresponding to each GWL were identified following the time-sampling methodology described by James et al. (2017) and applied in the IPCC AR6 (e.g., Nikula et al., 2018; Seneviratne et al., 2021). In this framework, for each GWL, we identified the period during which the 20-year running mean of the global mean surface temperature first exceeds the selected warming threshold relative to 1850–1900. The detailed implementation is described in Hauser et al. (2022). The GWL periods are listed in Table S1 in the Supplementary material.

Consistent with IPCC AR6, the GWLs are expressed relative to the pre-industrial baseline (1850–1900), whereas regional impacts are often interpreted relative to the modern reference period (1995–2014). The historical global warming between these two periods is approximately 0.94 °C according to IPCC (Ara Begum et al., 2022); this value is provided for reference only, as no baseline adjustment was applied in our analysis (James et al., 2017).

2.2. *Data selection and postprocess*

We employed two partially overlapping subsets of CMIP6 global climate models (GCMs), each identified in the literature as performing robustly over Central Europe. The first subset follows Palmer et al. (2023) (hereinafter the PLM subset), which was derived through a multi-criteria model performance evaluation based on large-scale circulation, temperature, and precipitation biases, and seasonal variability compared with observations and reanalyses. The second subset follows the selection of the ClimRisk project (https://www.climrisk.eu/), which provides high-resolution projections and risk assessments for Central Europe (further denoted as CR subset). The ClimRisk subset selection is based on Meitner et al. (2023) and combines several evaluation steps, taking into account temperature and precipitation biases, spatial pattern correlations with observations, the seasonal cycle, and circulation. The CR subset selection also accounts for the spread of future projections of changes in the variables used for evapotranspiration evaluation (https://www.climrisk.eu/). From the two model subsets (PLM and CR), we selected simulations for which the r1i1p1f1 ensemble member was available, or, where necessary, variants with the same initialization but different forcing indices (e.g., r1i1p1f2, r1i1p1f3). This step resulted in omitting the CESM2-WACCM model from the original PLM subset. In addition, we did not use the SSP126 scenario for the GFDL-ESM4 model because the simulation did not reach even the lowest considered GWL under the methodology we applied. GWL periods were derived from the mean near-surface air temperature (tas) of these simulations for all the available socio-economic scenarios listed in Table 1. Daily minimum (tasmin) and maximum (tasmax) temperature fields were interpolated onto a common 0.1° × 0.1° (~10 km) grid consistent with the E-OBS observational dataset using the CDO remapbil bilinear interpolation (Schulzweida, 2023). Subsequently, all simulations were bias-corrected using the Quantile Delta Mapping (QDM) method (Cannon et al., 2015), implemented via the cmethods Python package (Schwertfeger, 2025). QDM was selected because it is a relatively simple method to adjust biases across the full distribution which makes it suitable to study extreme values (Wang et al., 2016). QDM also preserves the model-projected climate change signal (Casanueva et al., 2020) which was important to study the impact of different GWLs. The E-OBS v30.0e dataset (Cornes et al., 2018) served as the reference for bias correction. We used 1980–2014 as the baseline period and applied the correction to the 2015–2100 projection period. The selected heat extreme indices were then calculated from the bias-corrected simulations for each GWL period. The results include values for the observed climate of the recent reference period (1995–2014) as well as projected values for the different GWLs. Fig. 2 shows a simplified workflow of the data postprocessing procedure.

Table 1. List of CMIP6 simulations used in this study. For each Global Climate Model (GCM), we provide corresponding modelling institution, ensemble member, and available Socio-economic scenarios, and indication of the subset in which the GCM is included: PLM (Palmer et al., 2023) and CR (ClimRisk; Meitner et al., 2023) or both (PLM/CR). For more details about CMIP6 simulations, see Eyring et al. (2016).

No	GCM	Institution	Ensemble member	Socio-economic scenarios	Subset
1	BCC-CSM2-MR	Beijing Climate Center (BCC, China)	r1i1p1f1	ssp126, ssp245, ssp370, ssp585	PLM
2	HadGEM3-GC31-MM	Met Office Hadley Centre (UK)	r1i1p1f3	ssp126, ssp585	PLM
3	CMCC-ESM2	Centro Euro-Mediterraneo sui Cambiamenti Climatici (CMCC, Italy)	r1i1p1f1	ssp126, ssp245, ssp370, ssp588	CR
4	MPI-ESM1-2-HR	Max Planck Institute for Meteorology (MPI-M, Germany)	r1i1p1f1	ssp126, ssp245, ssp370, ssp585	CR
5	TaiESM1	Research Center for Environmental Changes, Academia Sinica (Taiwan)	r1i1p1f1	ssp126, ssp245, ssp370, ssp585	CR

6	MRI-ESM2-0	Meteorological Research Institute (MRI, Japan)	r1i1p1f1	ssp126, ssp245, ssp370, ssp585	PLM/CR
7	GFDL-ESM4	NOAA Geophysical Fluid Dynamics Laboratory (GFDL, USA)	r1i1p1f1	ssp245, ssp370, ssp585	PLM/CR
8	EC-Earth3	EC-Earth Consortium (Europe)	r1i1p1f1	ssp126, ssp245, ssp370, ssp585	PLM/CR
9	CNRM-CM6-1-HR	Centre National de Recherches Météorologiques (CNRM) & Météo-France (France)	r1i1p1f2	ssp126, ssp585	PLM/CR

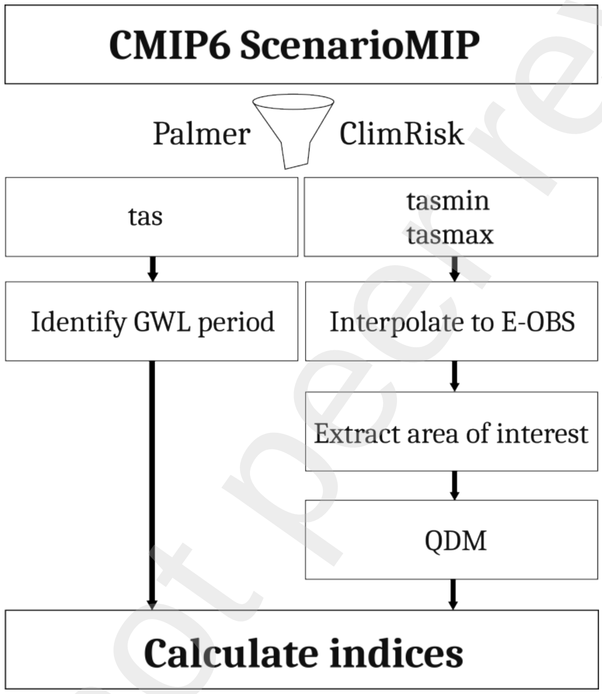

Fig. 2 Simplified workflow of the data postprocessing

2.3. *Selected heat extremes and derived statistics*

We assess the co-occurrence of selected daytime and nighttime heat extremes. We used the following indices calculated from daily maximum (T_{max}) and minimum temperature (T_{min}). Daytime extremes include:

- summer days (SD, $T_{max} \geq 25$ °C),
- hot days (HD, $T_{max} \geq 30$ °C),
- extremely hot days (EHD, $T_{max} \geq 35$ °C),

while nighttime extremes are represented by:

- tropical nights (TN, $T_{min} \geq 20$ °C).

The definitions of summer days and tropical nights follow the European Climate Assessment & Dataset (ECA&D, 2025). The hot day threshold is commonly used in Central Europe (Tomczyk et al., 2021), and we further extend the analysis to extremely hot days applied in impact-oriented heat assessments (U.S. EPA, 2025). Co-occurring events take place when a daytime and a nighttime extreme happen on the same day, forming the combinations TN+SD, TN+HD, and TN+EHD. Besides the number of co-occurrences, we also evaluate the maximum duration of these events as the maximum number of consecutive days with the co-occurrent events within each GWL period. We generated spatial maps for the ensemble means of the two model subsets (see Section 3.1), providing an overview of the spatial distribution of compound heat events and informing the selection of representative NUTS regions. For each selected NUTS region, we computed area-averaged values of mean co-occurrence frequency and maximum duration for individual simulations (see Section 3.2).

2.4. Influence of model and scenario on the number of co-occurrences

To compare the influence of the socio-economic scenario and individual models on the projected changes in co-occurring heat extremes, we employed the analysis of variance (Von Storch and Zwiers, 2002). This approach has been used before, especially in studies concerned with regional climate model simulations to investigate the uncertainty connected to driving and nested models (e.g., Dequé et al., 2007; Holtanová et al., 2014) The variance decomposition results in comparison of two components, related to scenario and model, and their interaction (or simply, the residuals). The F-test then enables assessment of whether the influence of each factor is statistically significant or not (we use the significance level of 5%). The calculations were performed using the aov function in the R environment (Chambers et al., 1992) and the results are shown in Fig. S7

3. Results

3.1. Spatial distribution of heat extreme co-occurrences

The spatial distribution of heat-extreme co-occurrences for the observational reference period (1995–2014, based on E-OBS) and for GWL1.5, GWL1.9, GWL2.0, and GWL2.7 °C were examined using the ensemble mean of the two CMIP6 subsets (Fig 3–4, Fig S1-S4), including all the simulations available (See Table 1). Not all SSP scenarios reach all warming levels during the studied period (Table S1), so the number of simulations varies across GWLs. We focus on the mean because it provides the clearest and most interpretable basis for regional decision-making. Other statistics (such as the range, standard deviation, or median) can offer additional insight, but they introduce more complexity, and one aim of this study is to provide results that are easy to understand and directly usable for adaptation planning, so we just focus on the mean here. For clarity of presentation, results for the TN+HD co-occurrence are shown in the main text (Fig. 3–4), while results for the other combinations are provided in the Supplement (Fig. S1–S4). This choice is motivated by similar magnitudes of TN+HD and TN+SD (both occurring more frequently than TN+EHD) and the greater relevance of hot days than summer days for impact assessments.

In the observational period, co-occurrence events are nearly absent across most of the domain for all three types of co-occurrence events, except in the south-eastern part, where the number of TN+HD is around 9–12 days per year, and the TN+SD is 12–15 days per year in some grids in the Pest County in Hungary (Fig. 3 and Fig S1). Note that in this area, the effect of the city of Budapest is high due to the urban heat island (UHI). Besides these higher values, small non-zero values appear only in warmer lowland regions, mainly around two other big cities, Vienna and Berlin, where the UHI is an important factor too (Fig. 3, Fig. S1 and Fig. S3). In case of the most extreme event, TN+EHD, there are only very small areas in the Danube–Tisza Interfluve in Hungary and near the capital, Budapest, with 1.5–3 days per year (Fig S3).

As GWLs increase, these areas are projected to expand, and the number of events increases in both model subsets. As expected, higher warming levels lead to larger spatial extents and higher frequencies of the co-occurrences (Fig. 4, Fig. S2 and Fig. S4). A clear expansion of the affected area appears between GWL1.9 and GWL2.0, where many locations begin to experience at least three co-occurrence days per year. With each warming step, existing hotspots intensify, and new hotspots emerge. Here, “hotspots” refer to areas that visibly stand out with higher values relative to their surroundings. This pattern is consistent across all types of co-occurrences. Because both model subsets were bias corrected using the same observational dataset, their overall spatial patterns are broadly similar (as the GCMs have coarser horizontal resolution than the EOBS, the bias correction results in adapting the main patterns of spatial variability from EOBS). Even so, the maps highlight how different warming levels and event types affect regions differently. In particular, hotspots for the most intense co-occurrence type (TN+EHD) appear in similar areas to those for milder types but show stronger spatial expansion at higher GWLs (Figure S4). Some parts of the domain show little or no increase in co-occurrences even at higher warming levels. These “safe spots” are mainly cooler, higher-elevation regions (see Fig. 1, which shows the orography). where heat-related extremes remain rare. Note that these regions may also face other climate-related hazards not studied here.

As we discussed in Section 2, we selected subregions to illustrate that our approach is applicable at different administrative levels to support decision-making. Besides social and economic arguments, we selected the regions using the spatial distribution maps presented in this section to represent different climatic conditions and diverse future projections of co-occurrences. The analyses for these NUTS regions indicated on Fig. 5–6, and Fig. S5–S8, are presented in Sections 3.2.

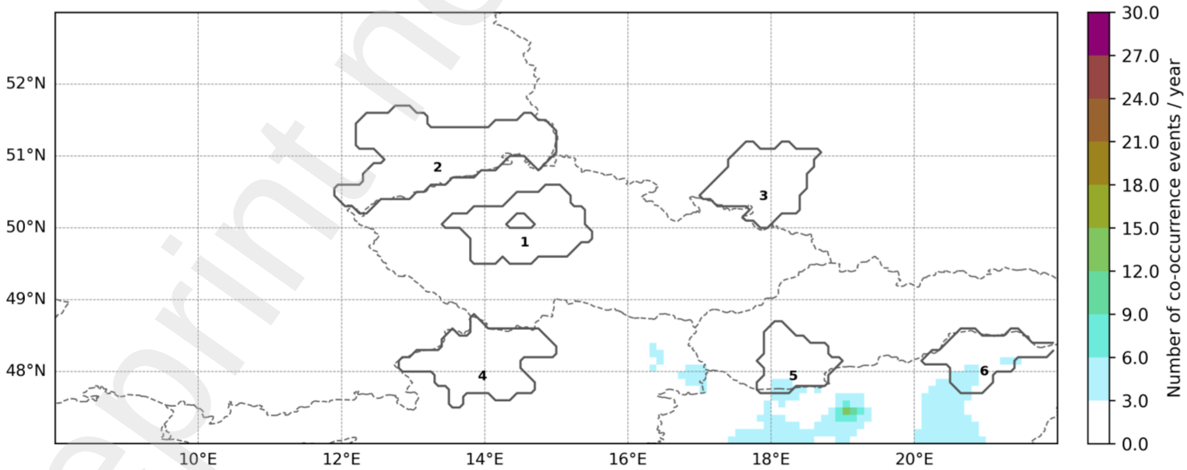

Fig. 3: Number of Tropical Night + Hot Day co-occurrence events derived from the E-OBS v30.0e observational dataset. Numbers denote selected NUTS regions (1: CZ020, 2: DED, 3: PL52, 4: AT31, 5: SK023, 6: HU311).

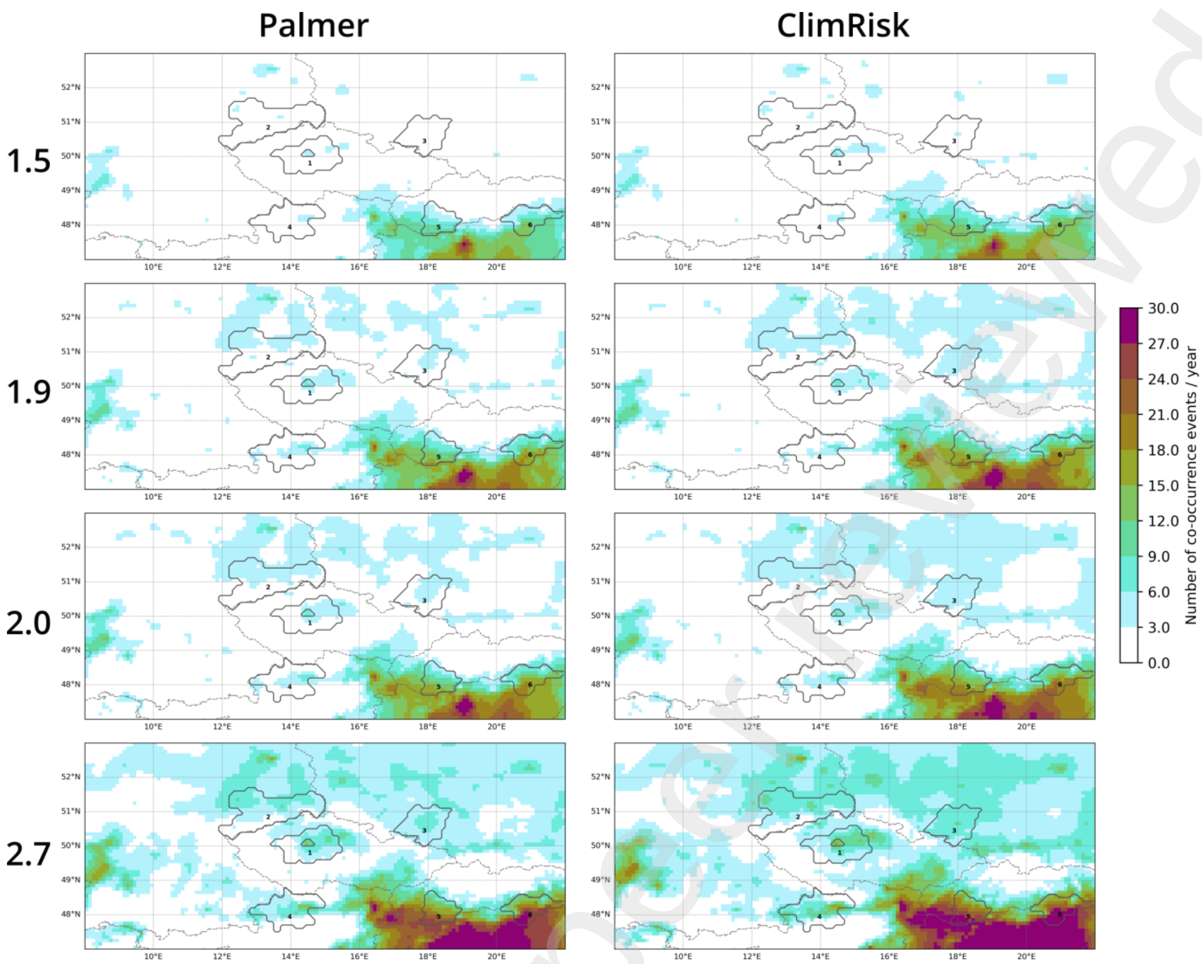

Fig. 4: Ensemble-mean annual number of Tropical Night + Hot Day co-occurrence events. Rows show Global Warming Levels (1.5, 1.9, 2.0 and 2.7 °C), and columns show the two model subsets (Palmer - PLM and ClimRisk - CR). Numbers denote selected NUTS regions (1: CZ020, 2: DED, 3: PL52, 4: AT31, 5: SK023, 6: HU311).

3.2. Area-mean co-occurrence characteristics in NUTS regions

The plots show the area-mean co-occurrence frequency for the selected NUTS for all model–scenario simulations across the four GWLs for the TN+HD (Fig. 5–6), TN+SD (Fig. S5–6) and TN+EHT (Fig. S7–8) co-occurrences. Each mark represents one simulation. Different colours indicate different models, and different marker shapes represent different scenarios. The annotations indicate whether a simulation belongs to the PLM subset, the CR subset, or both. For each NUTS region, the subset mean values (PLM mean and CR mean) are also shown.

The plots provide three perspectives: (1) the distribution of individual simulations (all the data points), which gives the full uncertainty range; (2) how the distribution changes with GWL; and (3) the subset means (PLM and CR), which provide simple, ready-to-use estimates for regional planning. These can serve as decision-relevant central estimates, while the spread, an inherent feature of multi-model climate projections, can be used to evaluate uncertainty or higher-risk outcomes. The inevitable presence and considerable magnitude of the spread highlight the importance of using a model ensemble rather than a single simulation. It reflects (i) structural differences between climate models, (ii) differences in scenario trajectories, and (iii) internal variability (Lehner and Deser, 2023).

Two consistent features emerge across the six NUTS regions. First, the spread between simulations generally increases with GWL, indicating that projections diverge more under stronger warming. Second, a higher emission scenario does not always produce a larger value at a given GWL; especially for lower GWLs, the SSP245 and SSP370 often project higher frequency of co-occurrences than SSP585 (Fig. 4). Differences in regional responses and internal variability imply that scenario "rank" does not simply map onto outcome magnitude at fixed global warming. A lower direct influence of the scenario choice on the co-occurrence frequencies is confirmed by the decomposition of the overall variance into the contributions from the models and scenarios (Fig. S9). The uncertainty is related mainly to the choice of the model. The influence of the socioeconomic scenario has a smaller effect, less than 10% in many cases and not more than 25% in any case. Our results are, in this regard, consistent with previous studies (e.g., Evin et al., 2024). However, we also show that the scenario influence increases with higher GWL (Fig. S9). Across the selected NUTS regions, the area-mean co-occurrence frequencies of TN+HD show pronounced regional contrasts (Fig. 5–6). The highest values are consistently projected for Hungary (HU311), in agreement with the spatial patterns, with Slovakia (SK023) also exhibiting relatively high frequencies (Fig. 6). These warmer regions additionally display the largest inter-model spread, indicating increased uncertainty under stronger warming. Both regions consistently exhibit the highest TN+HD frequencies among the analysed subregions. For Austria (AT31), model agreement is generally strong, with an overall range of about four days across simulations; however, the TaiESM1 model stands out as a clear outlier under GWL2.7, projecting substantially higher values than the rest of the ensemble (Fig. 5). The German (DED) and Czech (CZ020) regions show very similar distributions of simulations and subset means, indicating comparable regional responses to increasing global warming (Fig. 5).

For co-occurrences of TN+SD, regional differences are more pronounced, reflecting the higher absolute frequencies of these events (Fig. S5–6). The NUTS region selected for Poland (PL52) consistently exhibits higher values than CZ020 across all GWLs, illustrating that regional contrasts can be substantial and would be obscured in domain-wide or country averages (Fig. S5). This highlights the importance of analysing impacts at the administrative scales relevant for adaptation planning. Agreement between the PLM and CR subsets is strongest for the DED region. In most regions, differences between the two subset means are typically on the order of one to two days per year, while larger differences occur for Hungary (HU311) and Slovakia (SK023); however, these regions also show two to three times higher projected TN+SD frequencies overall.

Co-occurrences of TN+EHT are projected to remain rare in most regions (Fig. S7–8), with typically only one to two days per year even under GWL2.7, corresponding to warming levels associated with current policy trajectories. Hungary (HU311) and Slovakia (SK023) form clear exceptions, with substantially higher projected frequencies (Fig. S8). This again demonstrates that Central Europe–wide assessments may not be sufficient for detailed risk evaluation, as large differences can arise even within a relatively small domain, reinforcing the need for subregional analyses aligned with decision-making levels.

Fig. 5 Area-averaged future annual number of Tropical Night + Hot Day co-occurrence events for CZ020 (top), DED (middle), PL52 (bottom) NUTS regions under four global warming levels (GWL 1.5 °C, 1.9 °C, 2.0 °C, and 2.7 °C). Coloured symbols represent individual CMIP6 models and marker shapes represent socio-economic scenarios. Dashed pink line indicates the observed reference value using E-OBS v30.0e. Green and purple star symbols denote subset-mean values for the PLM subset and CR subset simulations, respectively.

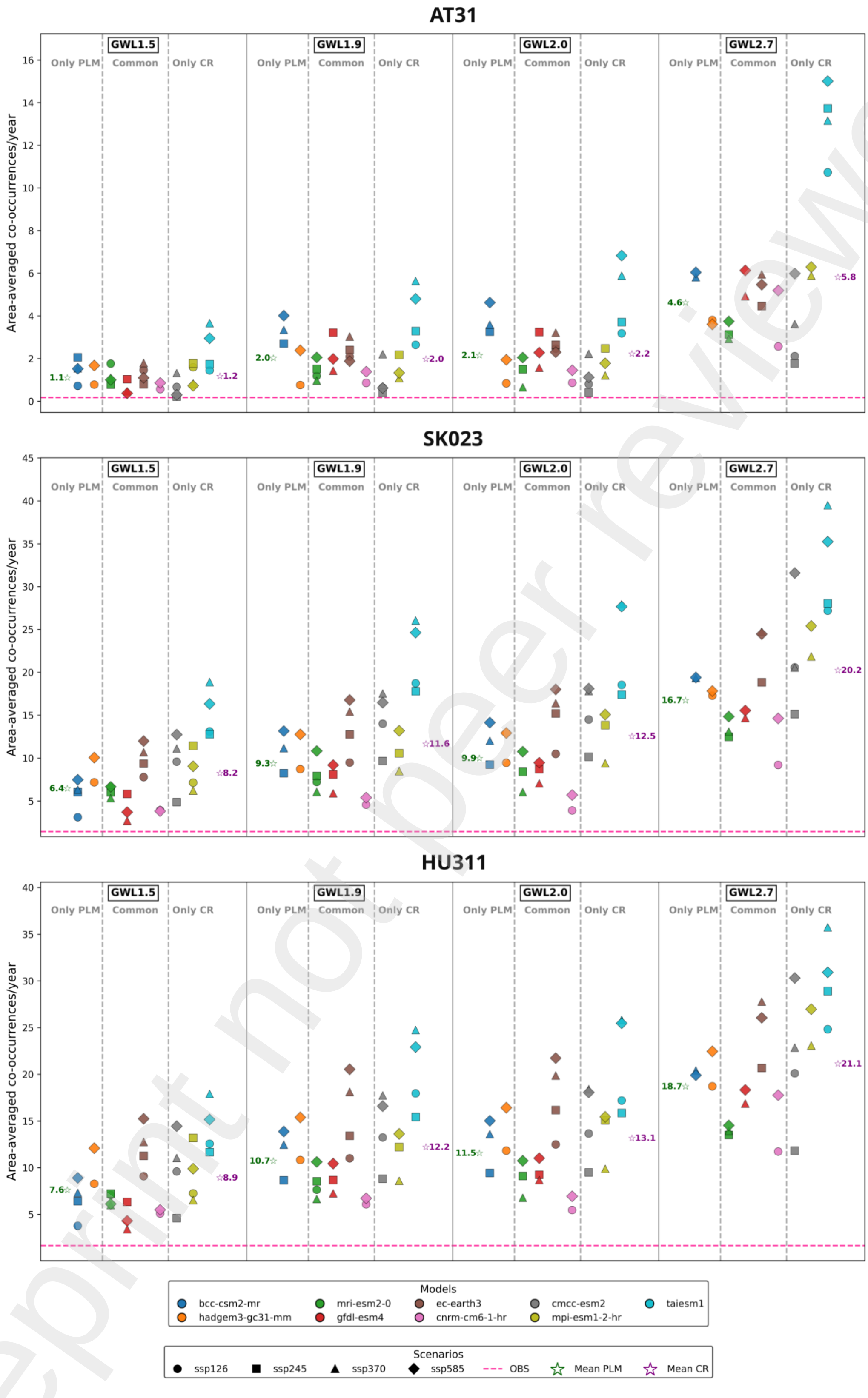

AT31
SK023
HU311
GWL1.5
GWL1.9
GWL2.0
GWL2.7
Only PLM
Common
Only CR
Area-averaged co-occurrences/year
Models
bcc-csm2-mr
hadgem3-gc31-mm
mri-esm2-0
gfdl-esm4
ec-earth3
cnrm-cm6-1-hr
cmcc-esm2
mpi-esm1-2-hr
taiesm1
Scenarios
ssp126
ssp245
ssp370
ssp585
OBS
Mean PLM
Mean CR

437

Fig. 6 Area-averaged future annual number of Tropical Night + Hot Day co-occurrence events for AT31 (top), SK023 (middle), HU311 (bottom) NUTS regions under four global warming levels (GWL 1.5 °C, 1.9 °C, 2.0 °C, and 2.7 °C). Coloured symbols represent individual CMIP6 models and marker shapes represent socio-economic scenarios. Dashed pink line indicates the observed reference value using E-OBS v30.0e. Green and purple star symbols denote subset-mean values for the PLM subset and CR subset simulations, respectively.

So far, we have focused on the mean frequencies of co-occurring extreme events under different GWLs. Another perspective is provided by the analysis of the duration of co-occurrences, summarised in Table 2 and complemented by the individual model–scenario results presented in Tables S2–S19. The duration metric captures the maximum annual length of consecutive co-occurrences of tropical nights with summer days and hot or extremely hot days. Table 2 shows that both the mean and the overall maximum annual longest durations for a GWL period increase with rising global warming levels across all analysed NUTS regions. The values are the mean of the two studied subsets, PLM or CR. Co-occurrences of TN+EHD, exhibit the strongest relative increases with higher GWLs. The Slovakian and Hungarian NUTS regions, SK023 and HU311, consistently display the longest durations and highest maxima, identifying them as regional hotspots of heat risk, while alpine and more western regions show lower durations but still substantial relative increases. Maximum durations generally increase more rapidly than mean values, highlighting an increasing likelihood of exceptionally persistent heat episodes. Across all regions and warming levels, the CR subset yields systematically higher duration estimates than PLM, with differences widening under stronger warming.

The analysis of individual model–scenario combinations in Table S2–S19 provides further insight into the behavior of maximum durations. Our results are consistent with the notion that extremes are strongly influenced by internal climate variability, which modulates the forced warming signal underlying temperature extremes. In this context, it is not surprising that, in many cases, the maximum durations are identical across different GWLs. This behavior is partly related to the overlapping time periods associated with individual GWLs (Table S1) and reflects the fact that the longest-lasting co-occurrences do not necessarily occur at the highest levels of global warming but may arise earlier. Furthermore, instances in which higher GWLs or stronger forcing scenarios exhibit shorter maximum durations may be linked to changes in day-to-day temperature variability. Increased variability can lead to more frequent or more intense extreme days, but also to greater temporal fragmentation of events, resulting in more frequent interruptions and, consequently, shorter continuous durations. A detailed investigation of the mechanisms governing changes in variability and event persistence is beyond the scope of this study.

Table 2 Mean and maximum of the annual longest durations (in days) of consecutive co-occurrences types (TN+SD as tropical night and summer day, TN+HD as tropical night and hot day and TN+EHD as torpical night and extreme hot day) within 20-year periods corresponding to the given global warming level (GWL), shown for the selected NUTS regions. The mean represents the average of the annual maximum durations over the 20-year period, while the maximum represents the largest annual maximum duration within that period. Values are shown as subset means (PLM and CR); individual model–scenario simulations are provided in the Supplementary Material Table S2–S19).

NUTS region	**Co-oc. type**	**Observed mean**	**Subset**	**GWL1.5 mean**	**GWL1.9 mean**	**GWL2.0 mean**	**GWL2.7 mean**	**GWL1.5 max**	**GWL1.9 max**	**GWL2.0 max**	**GWL2.7 max**
DED	TN+HD	0.13	PLM	0.91	1.42	1.53	2.27	3.89	5.54	5.43	6.87
			CR	0.98	1.44	1.57	2.71	4.39	5.88	5.91	9.57
	TN+EHD	0.06	PLM	0.44	0.72	0.79	1.28	2.32	3.46	3.59	4.8
			CR	0.59	0.88	0.97	1.76	2.98	4.2	4.25	7.62
	TN+SD	0.14	PLM	0.97	1.53	1.64	2.45	3.99	5.69	5.76	7.27
			CR	1.03	1.54	1.67	2.86	4.51	5.99	6.1	9.82
CZ020	TN+HD	0.12	PLM	0.85	1.4	1.48	2.38	3.81	5.66	5.77	6.9
			CR	0.96	1.39	1.5	2.85	4.42	5.46	5.6	9.29
	TN+EHD	0.03	PLM	0.49	0.84	0.89	1.5	2.85	4.06	4.22	4.68
			CR	0.64	0.95	1.03	2.01	3.56	4.28	4.41	7.59
	TN+SD	0.12	PLM	0.9	1.49	1.58	2.5	3.89	5.99	6.16	7.15
			CR	1	1.47	1.59	2.98	4.54	5.64	5.75	9.49
PL52	TN+HD	0.14	PLM	0.98	1.55	1.63	2.64	4.04	5.57	5.81	7.25
			CR	1.23	1.73	1.87	3.18	5.07	6.35	6.64	10.32
	TN+EHD	0.03	PLM	0.51	0.85	0.89	1.57	2.74	4.36	4.45	4.92
			CR	0.76	1.11	1.2	2.12	3.6	5.04	5.19	7.41
	TN+SD	0.15	PLM	1.02	1.62	1.7	2.79	4.25	5.87	6.13	7.68
			CR	1.28	1.8	1.95	3.36	5.36	6.67	6.94	10.86
AT31	TN+HD	0.14	PLM	0.72	1.17	1.25	2.27	3.39	4.08	4.2	6.05
			CR	0.72	1.1	1.22	2.72	3.71	4.1	4.36	7.3
	TN+EHD	0.01	PLM	0.31	0.47	0.52	1	1.99	2.35	2.46	3.53
			CR	0.41	0.59	0.67	1.61	2.52	2.8	2.94	5.05
	TN+SD	0.18	PLM	0.83	1.37	1.47	2.63	3.64	4.69	4.95	6.82
			CR	0.81	1.27	1.4	3.05	3.98	4.52	4.84	7.93
SK023	TN+HD	0.88	PLM	2.98	4.21	4.43	6.49	9.28	11.66	12.3	15.17
			CR	3.86	5.17	5.54	8.53	11.82	15.09	15.77	21.67
	TN+EHD	0.42	PLM	1.79	2.61	2.75	4.23	6.43	7.84	8.16	10.19
			CR	2.76	3.69	3.96	6.14	8.91	11.31	11.73	15.61
	TN+SD	0.89	PLM	3.02	4.27	4.49	6.63	9.3	11.79	12.43	15.35
			CR	3.89	5.22	5.6	8.66	11.83	15.17	15.85	21.75
HU311	TN+HD	1.03	PLM	3.35	4.67	5.05	7.12	10.97	13.18	13.89	15.95
			CR	4.1	5.42	5.88	8.67	13.45	16.03	16.78	21.57
	TN+EHD	0.33	PLM	1.76	2.63	2.83	4.1	7.08	8.49	9.06	10.44
			CR	2.64	3.63	3.9	5.76	9.72	11.65	12.1	15.29
	TN+SD	1.11	PLM	3.45	4.82	5.21	7.38	11	13.33	14.07	16.85
			CR	4.16	5.53	5.99	8.91	13.48	16.13	16.9	22.19

Discussion and conclusion

We applied the Global Warming Level (GWL) framework for the first time to assess how the co-occurrence of elevated daytime and nighttime temperatures is modelled to evolve over Central Europe by the current generation of GCMs. The explicit focus on co-occurring heat extremes based on both minimum and maximum temperature advances climate risk assessment, as such events limit nighttime recovery and amplify cumulative heat stress during prolonged episodes.

A key contribution of this study is the combination of policy-relevant global warming levels with aggregation of impacts to NUTS administrative regions, directly aligning projections with decision-making structures used in climate risk management. While most GWL studies focus on normative temperature thresholds such as 1.5 °C and 2.0 °C, these are not consistent with the warming implied by current policies. By complementing these targets with warming levels derived from policy-consistent temperature estimates, we assess co-occurring heat risk under conditions that regions are more likely to face without stronger mitigation. Presenting results at the NUTS level further demonstrates that heat risk varies substantially between neighbouring administrative units, confirming that domain-wide or national averages are insufficient for adaptation planning. Together, policy-relevant GWLs and administrative-scale aggregation provide decision-ready climate information linking global mitigation ambition with regional adaptation needs. To enhance practical usability, NUTS-level projections for six Central European countries are made publicly available through an open repository (Szabó et al., 2026), enabling regional authorities and climate service providers to directly access and apply the results in adaptation planning.

A limitation of the GWL framework is that it conditions impacts on temperature thresholds without explicitly addressing when those thresholds are reached. Timing is highly relevant for adaptation planning but introduces additional uncertainty related to emission pathways and internal variability. Emerging approaches integrating probabilistic or machine-learning estimates of GWL timing (Barnes et al., 2025) offer promising directions for future work. Methodological uncertainty also arises from bias correction. Quantile delta mapping (QDM) corrects systematic biases relative to an observational reference but does not modify future tail behaviour beyond that simulated by the underlying model. Thus, the credibility of projected extremes ultimately depends on the model's ability to represent extreme temperature characteristics. QDM is nevertheless widely used and considered appropriate for temperature extremes (Wang et al., 2016; Casanueva et al., 2020). Further, the E-OBS dataset, used as observational reference, provides spatial consistency across Europe but carries uncertainties related to station density and interpolation, particularly in complex terrain (Dosio, 2016; Kalmár et al., 2023). The use of bias-corrected CMIP6 GCM output with statistical downscaling is consistent with previous GWL-based impact studies (Ruosteenoja et al., 2023a,b) and enables robust sampling of structural model uncertainty while maintaining methodological transparency. However, global models remain limited in representing regional-scale processes. Regional climate model studies over Europe (Vautard et al., 2014; Jacob et al., 2018; Kjellström et al., 2018; Pfeifer et al., 2019; Diez-Sierra et al., 2023) demonstrate that higher-resolution simulations can refine the spatial structure and intensity of extremes. Applying the present framework to forthcoming EURO-CORDEX Phase 2 simulations represents an important next step.

Across all regions, ensemble spread increases with higher warming levels. Variance decomposition shows that model choice dominates uncertainty, whereas socio-economic scenario choice contributes comparatively little at lower GWLs and remains secondary even at higher warming levels. This confirms an advantage of the GWL approach: conditioning impacts on temperature thresholds reduces scenario dependence relative to fixed time-slice analyses (Evin et al., 2024), although scenario influence may grow at higher warming levels. Projected changes in co-occurring heat extremes are not strongly governed by model climate sensitivity. Models with similar equilibrium climate sensitivity produce markedly different regional responses, while some high-sensitivity models show moderate increases. For example, TaiESM1 projects substantially stronger increases in certain co-occurrence metrics, largely driven by a pronounced rise in daytime maximum temperature (not shown), whereas HadGEM3-GC31-MM, despite high climate sensitivity, shows comparatively moderate responses. These contrasts highlight the importance of regional processes and internal variability for the co-occurring temperature extremes. Comparison of the two performance-informed subsets reinforces this conclusion. The CR subset generally projects higher increases in frequency and duration than the PLM subset, particularly at higher warming levels and in regions with strong responses such as Hungary. Although TaiESM1 contributes to this tendency, subset differences are not attributable to a single model and likely reflect differences in model formulation and regional process representation. This underscores that performance-based model selection is necessary but does not eliminate uncertainty, especially for compound extremes where small differences in T_{max} or T_{min} can lead to large differences in co-occurrence metrics. Beyond mean frequency changes, event-duration analysis reveals a disproportionate increase in persistent co-occurring heat-event periods. Maximum annual durations generally increase faster than mean values, indicating rising likelihood of prolonged heat stress. At the same time, internal variability strongly modulates extreme persistence, and the longest events do not necessarily occur at the highest warming levels. Variability-driven fragmentation of extreme days may partly explain cases of shorter maximum durations at higher GWLs, warranting further investigation.

In conclusion, co-occurring heat extremes involving simultaneous daytime and nighttime heat intensify rapidly with global warming across Central Europe, including warming levels consistent with current national policies. Relatively small increments in global mean temperature can produce disproportionate increases in both frequency and persistence, with pronounced regional contrasts. By integrating policy-relevant

GWLs and NUTS-scale aggregation, this study provides climate information that directly supports region-specific adaptation planning. While uncertainty remains substantial—primarily driven by model differences and internal variability—the GWL framework clarifies plausible risk ranges and reduces scenario uncertainty. Extending this approach with higher-resolution regional climate simulations will further enhance its value for next-generation climate services and climate risk management.

Acknowledgement

The authors are grateful to the Johannes Amos Comenius Operational Programme (OP JAC), project No. CZ.02.01.01/00/22_008/0004605 – Natural and Anthropogenic Geohazards, which supported this research. We acknowledge the E-OBS dataset and the data providers in the ECA&D project. We thank the World Climate Research Programme's Working Group on Coupled Modelling for coordinating CMIP and the climate modeling groups for producing and sharing their model output. The CMIP data used in this study were replicated and made available by the Deutsches Klimarechenzentrum (DKRZ) and the Centre for Environmental Data Analysis (CEDA).

Declaration of generative AI and AI-assisted technologies in the manuscript preparation process

During the preparation of this work, the authors used AI-assisted tools to improve language and readability. After using these tools, the authors reviewed and edited the content as needed and take full responsibility for the content of the published article.

Reference list

Abramowitz G, Herger N, Gutmann E, Hammerling D, Knutti R, Leduc M, Schmidt GA (2019) ESD reviews: Model dependence in multi-model climate ensembles: Weighting, sub-selection and out-of-sample testing. Earth System Dynamics 10(1): 91–105. https://doi.org/10.5194/esd-10-91-2019

Ara Begum R, Lempert R, Ali E, Benjaminsen TA, Bernauer T, Cramer W, Cui X, Mach K, Nagy G, Stenseth NC, Sukumar R, Wester P (2022) Point of Departure and Key Concepts. In: Pörtner H-O, Roberts DC, Tignor M, Poloczanska ES, Mintenbeck K, Alegría A, Craig M, Langsdorf S, Löschke S, Möller V, Okem A, Rama B (eds) Climate Change 2022: Impacts, Adaptation and Vulnerability. Contribution of Working Group II to the Sixth Assessment Report of the Intergovernmental Panel on Climate Change. Cambridge University Press, Cambridge, UK and New York, NY, USA, pp 121–196. https://doi.org/10.1017/9781009325844.003

Barnes EA, Diffenbaugh NS, Seneviratne SI (2024) Combining climate models and observations to predict the time remaining until regional warming thresholds are reached. Environmental Research Letters 20(1): 014008. https://doi.org/10.1088/1748-9326/ad91ca

Becsi B, Formayer H (2024) Linking local climate scenarios to global warming levels: applicability, prospects and uncertainties. Environmental Research: Climate 3: 045003. https://doi.org/10.1088/2752-5295/ad574e

Cannon AJ, Sobie SR, Murdock TQ (2015) Bias correction of GCM precipitation by quantile mapping: How well do methods preserve changes in quantiles and extremes? Journal of Climate 28(17): 6938–6959. https://doi.org/10.1175/JCLI-D-14-00754.1

Casanueva, A, Herrera, S, Iturbide, M, Lange, S, Jury, M, Dosio, A, Maraun, D, Gutiérrez, JM (2020). Testing bias adjustment methods for regional climate change applications under observational uncertainty and resolution mismatch. Atmospheric Science Letters, 21(7). https://doi.org/10.1002/asl.978

Chambers JM, Freeny A, Heiberger RM (1992) Analysis of variance; designed experiments. In: Chambers JM, Hastie TJ (eds) Statistical Models in S. Wadsworth & Brooks/Cole.

CAT (2024) Climate Action Tracker Global Update: As the climate crisis worsens, the warming outlook stagnates. Climate Analytics, NewClimate Institute & The Energy and Resources Institute (TERI). https://climateactiontracker.org/publications/cat-global-update-as-the-climate-crisis-worsens-the-warming-outlook-stagnates

Cornes RC, van der Schrier G, van den Besselaar EJM, Jones PD (2018) An ensemble version of the E-OBS temperature and precipitation data sets. Journal of Geophysical Research: Atmospheres 123(17): 9391–9409. https://doi.org/10.1029/2017JD028200

Denissen JMC, Teuling AJ, Koirala S, Reichstein M, Balsamo G, Vogel MM, Yu X, Orth R (2024) Intensified future heat extremes linked with increasing ecosystem water limitation. Earth System Dynamics 15(3): 717–734. https://doi.org/10.5194/esd-15-717-2024

Déqué M (2007) Frequency of precipitation and temperature extremes over France in an anthropogenic scenario: model results and statistical correction according to observed values. Glob Planet Change 57:16–26. https://doi.org/10.1016/j.gloplacha.2006.11.030

Diez-Sierra J, Iturbide M, Fernández J, Milovac J, Gutiérrez JM, Cimadevilla E, Kjellström E, Bülow K, Horányi A, Pérez A, Baño-Medina J, Ahrens B, Alias A, Ashfaq M, Bukovsky M, Buonomo E, … Rechid D (2023) Consistency of the regional response to global warming levels from CMIP5 and CORDEX projections. Climate Dynamics 61: 4047–4060. https://doi.org/10.1007/s00382-023-06790-y

Dosio A (2016) Projections of climate change indices of temperature and precipitation from an ensemble of bias-adjusted high-resolution EURO-CORDEX regional climate models. Journal of Geophysical Research: Atmospheres 121(10): 5488–5511. https://doi.org/10.1002/2015JD024411

Dosio A, Mentaschi L, Fischer EM, Wyser K (2018) Extreme heat waves under 1.5 °C and 2 °C global warming. Environmental Research Letters 13(5): 054006. https://doi.org/10.1088/1748-9326/aab827

European Climate Assessment & Dataset (ECA&D) (2025) Indices of extremes (indices dictionary). Royal Netherlands Meteorological Institute (KNMI). https://www.ecad.eu/indicesextremes/indicesdictionary.php

Eurostat (2024). Regions in the European Union — Nomenclature of Territorial Units for Statistics (NUTS), 2024 edition. Eurostat manual KS-GQ-23-010. European Commission.

Eyring V, Bony S, Meehl GA, Senior CA, Stevens B, Stouffer RJ, Taylor KE (2016) Overview of the Coupled Model Intercomparison Project Phase 6 (CMIP6) experimental design and organization. Geoscientific Model Development 9(5): 1937–1958. https://doi.org/10.5194/gmd-9-1937-2016

Evin, G, Ribes, A, Corre, L. (2024) Assessing CMIP6 uncertainties at global warming levels. Clim Dyn **62**, 8057–8072 https://doi.org/10.1007/s00382-024-07323-x

Forzieri G, Cescatti A, Batista e Silva F, Feyen L (2017) Increasing risk over time of weather-related hazards to the European population: A data-driven approach. Global Environmental Change 44: 39–50. https://doi.org/10.1016/j.gloenvcha.2017.03.008

Gallo E, Quijal-Zamorano M, Méndez Turrubiates RF, Tonne C, Basagaña X, Achebak H, Ballester J (2024) Heat-related mortality in Europe during 2023 and the role of adaptation in protecting health. Nature Medicine. https://doi.org/10.1038/s41591-024-03186-1

Gasparrini A, Guo Y, Sera F, Vicedo-Cabrera AM, Huber V, Tong S, Armstrong B (2017) Projections of temperature-related excess mortality under climate change scenarios. The Lancet Planetary Health 1(9): e360–e367. https://doi.org/10.1016/S2542-5196(17)30156-0

Guo L, Jiang Z, Chen D, Le Treut H, Li L (2020) Projected precipitation changes over China for global warming levels at 1.5 °C and 2 °C in an ensemble of regional climate simulations: impact of bias correction methods. Climatic Change 162(2): 623–643. https://doi.org/10.1007/s10584-020-02841-z

Hauser et al. (2022). Transient global warming levels for CMIP5 and CMIP6 (v0.3.0). Zenodo. https://doi.org/10.5281/zenodo.7390473

Hausfather Z, Marvel K, Schmidt GA, Nielsen-Gammon JW, Zelinka M (2022) Climate simulations: recognize the 'hot model' problem. Nature 605(7908): 26–29. https://doi.org/10.1038/d41586-022-01192-2

He C, Kim H, Hashizume M, Lee W, Honda Y, Kim SE, Kinney PL, Schneider A, Zhang Y, Zhu Y, Zhou L, Chen R, Kan H (2022) The effects of night-time warming on mortality burden under future climate change scenarios: a modelling study. The Lancet Planetary Health 6(8): e648–e657. https://doi.org/10.1016/S2542-5196(22)00139-5

Holtanova, E, Kalvova, J, Pisoft, P, Miksovsky, J (2014) Uncertainty in regional climate model outputs over the Czech Republic: the role of nested and driving models. International Journal of Climatology, 34:1, 27–35, https://doi.org /10.1002/joc.3663

IPCC (2023) Climate Change 2023: Synthesis Report. Contribution of Working Groups I, II and III to the Sixth Assessment Report of the Intergovernmental Panel on Climate Change [Core Writing Team, H. Lee and J. Romero (eds.)]. IPCC, Geneva, Switzerland, pp. 35-115, https://doi.org/10.59327/IPCC/AR6-9789291691647

Jacob D, Kotova L, Teichmann C, Sobolowski SP, Vautard R, Donnelly C, Koutroulis AG, Grillakis MG, Tsanis IK, Damm A, Sakalli A, van Vliet MTH (2018) Climate impacts in Europe under +1.5 °C global warming. Earth's Future 6(2): 264–285. https://doi.org/10.1002/2017EF000710

James RA, Washington R, Schleussner C-F, Rogelj J, Conway D (2017) Characterizing half-a-degree difference: A review of methods for identifying regional climate responses to global warming targets. WIREs Climate Change 8: e457. https://doi.org/10.1002/wcc.457

Kalmár T, Kristóf E, Hollós R, Pieczka I, Pongrácz R (2023) Quantifying uncertainties related to observational datasets used as reference for regional climate model evaluation over complex topography — a case study for the wettest year 2010 in the Carpathian region. Theoretical and Applied Climatology 153(1-2): 807–828. https://doi.org/10.1007/s00704-023-04491-4

King AD, Karoly DJ (2017) Climate extremes in Europe at 1.5 and 2 degrees of global warming. Environmental Research Letters 12(11): 114031. https://doi.org/10.1088/1748-9326/aa8e2c

Kjellström, E., Nikulin, G., Strandberg, G., Christensen, O. B., Jacob, D., Keuler, K., Lenderink, G., van Meijgaard, E., Schär, C., Somot, S., Sørland, S. L., Teichmann, C., and Vautard, R.: European climate change at global mean temperature increases of 1.5 and 2 °C above pre-industrial conditions as simulated by the EURO-CORDEX regional climate models, Earth Syst. Dynam., 9, 459–478, https://doi.org/10.5194/esd-9-459-2018, 2018.

Knutti R (2008) Should we believe model predictions of future climate change? Philosophical Transactions of the Royal Society A 366: 4647–4664. https://doi.org/10.1098/rsta.2008.0169

Lehner, F and Deser, C (2023) Origin, importance, and predictive limits of internal climate variability. Environmental Research: Climate, 2(2), 023001. https://doi.org/10.1088/2752-5295/accf30

Lhotka O, Kyselý J, Farda A (2018) Climate change scenarios of heat waves in Central Europe and their uncertainties. Theoretical and Applied Climatology 131(3-4): 1043–1054. https://doi.org/10.1007/s00704-016-2031-3

Liu J, Kim H, Hashizume M, Lee W, Honda Y, Kim SE, He C, Kan H, others (2025) Nonlinear exposure–response associations of daytime, nighttime, and day–night compound heatwaves with mortality amid climate change. Nature Communications 16: 635. https://doi.org/10.1038/s41467-025-56067-7

Matthews TKR, Wilby RL, Murphy C (2017) Communicating the deadly consequences of global warming for human heat stress. Proceedings of the National Academy of Sciences 114(15): 3861–3866. https://doi.org/10.1073/pnas.1617526114

Meehl GA, Senior CA, Eyring V, Flato G, Lamarque JF, Stouffer RJ, Schlund M (2020) Context for interpreting equilibrium climate sensitivity and transient climate response from the CMIP6 Earth system models. Science Advances 6(26): eaba1981. https://doi.org/10.1126/sciadv.aba1981

Meitner J, Štěpánek P, Skalák P, Dubrovský M, Lhotka O, Penčevová R, Zahradníček P, Farda A, Trnka M (2023) Validation and selection of a representative subset from the ensemble of EURO-CORDEX EUR11 regional climate model outputs for the Czech Republic. Atmosphere 14: 1442. https://doi.org/10.3390/atmos14091442

Merrifield AL, Brunner L, Lorenz R, Humphrey V, Knutti R (2023) Climate model Selection by Independence, Performance, and Spread (ClimSIPS v1.0.1) for regional applications. Geoscientific Model Development 16(16): 4715–4747. https://doi.org/10.5194/gmd-16-4715-2023

Nikulin G, Lennard C, Dosio A, Kjellström E, Chen Y, Hänsler A, Kupiainen M, Laprise R, Mariotti L, Maule CF, van Meijgaard E, Panitz H-J, Scinocca JF, Somot S (2018) The effects of 1.5 and 2 degrees of global warming on Africa in the CORDEX ensemble. Environmental Research Letters 13(6): 065003. https://doi.org/10.1088/1748-9326/aab1b1

Palmer TE, McSweeney CF, Booth BBB, Priestley MDK, Davini P, Brunner L, Borchert L, Menary MB (2023) Performance-based sub-selection of CMIP6 models for impact assessments in Europe. Earth System Dynamics 14(2): 457–483. https://doi.org/10.5194/esd-14-457-2023

Pfeifer S, Rechid D, Reuter M, Viktor E, Jacob D (2019) 1.5°, 2°, and 3° global warming: visualizing European regions affected by multiple changes. Regional Environmental Change 19(6): 1777–1786. https://doi.org/10.1007/s10113-019-01496-6

Reifen, C., & Toumi, R. (2009). Climate projections: Past performance no guarantee of future skill?. Geophysical Research Letters, 36(13). https://doi.org/10.1029/2009GL038082

Ripple WJ, Wolf C, Mann ME, Rockström J, Gregg JW, Xu C, Gleick PH (2025) The 2025 state of the climate report: A planet on the brink. BioScience 75(12): 1016–1027. https://doi.org/10.1093/biosci/biaf149

Ruosteenoja K, Jylhä K (2023)a Average and extreme heatwaves in Europe at 0.5–2.0 °C global warming levels in CMIP6 model simulations. Climate Dynamics 61(9-10): 4259–4281. https://doi.org/10.1007/s00382-023-06798-4

Ruosteenoja K, Jylhä K (2023)b Heatwave projections for Finland at different levels of global warming derived from CMIP6 simulations. Geofysica 58(1): 47–75. https://helda.helsinki.fi/handle/10138/178406

Schleussner C-F, Lissner TK, Fischer EM, Wohland J, Perrette M, Golly A, Rogelj J, Childers K, Schewe J, Frieler K, Mengel M, Hare W, Schaeffer M (2016) Differential climate impacts for policy-relevant limits to global warming: the case of 1.5 °C and 2 °C. Earth System Dynamics 7(2): 327–351. https://doi.org/10.5194/esd-7-327-2016

Schulzweida, Uwe. (2023) CDO User Guide (2.3.0). Zenodo. https://doi.org/10.5281/zenodo.10020800

Seneviratne SI, Donat MG, Pitman AJ, Knutti R, Wilby RL (2016) Allowable CO_2 emissions based on regional and impact-related climate targets. Nature 529(7587): 477–483. https://doi.org/10.1038/nature16542

Seneviratne SI, Hauser M (2020) Regional climate sensitivity of climate extremes in CMIP6 vs CMIP5 multimodel ensembles. Earth's Future 8(9): e2019EF001474. https://doi.org/10.1029/2019EF001474

Seneviratne SI, Zhang X, Adnan M, Badi W, Dereczynski C, Di Luca A, Ghosh S, Iskandar I, Kossin J, Lewis S, Otto F, Pinto I, Satoh M, Vicente-Serrano SM, Wehner M, Zhou B (2021) Weather and climate extreme events in a changing climate. In: Masson-Delmotte V, Zhai P, Pirani A, Connors SL, Péan C, Berger S, Caud N, Chen Y, Goldfarb L, Gomis MI, Huang M, Leitzell K, Lonnoy E, Matthews JBR, Maycock TK, Waterfield T, Yelekçi O, Yu R, Zhou B (eds) Climate Change 2021: The Physical Science Basis. Contribution of Working Group I to the Sixth Assessment Report of the Intergovernmental Panel on Climate Change. Cambridge University Press, Cambridge, UK and New York, NY, USA, pp 1513–1766. https://doi.org/10.1017/9781009157896.013

Sherwood S, Webb M, Annan J, Armour K, Forster P, Hargreaves J, Hegerl G, Klein S, Marvel K, Rohling E, Watanabe M, Andrews T, Braconnot P, Bretherton C, Foster G, Hausfather Z, von der Heydt AS, Knutti R, Mauritsen T, Norris J (2020) An assessment of Earth's climate sensitivity using multiple lines of evidence. Reviews of Geophysics 58. https://doi.org/10.1029/2019RG000678

Schwertfeger, BT (2025). btschwertfeger/python-cmethods: v2.3.2 (v2.3.2). Zenodo. https://doi.org/10.5281/zenodo.17606049

Szabó, AI, Holtanová, E, Belda, M (2026) Projections of co-occuring heat extremes in Central Europe at policy-relevant global warming levels (v1). Zenodo https://doi.org/10.5281/zenodo.18629469

Szewczyk W, Mongelli I, Ciscar J-C (2021) Heat stress, labour productivity and adaptation in Europe – a regional and occupational analysis. Environmental Research Letters 16(10): 105002. https://doi.org/10.1088/1748-9326/ac24cf33917051

Tomczyk AM, Bednorz E, Półrolniczak M, Kolendowicz L (2021) Climatological characteristics of hot days over Central Europe in 1951–2018. International Journal of Climatology 41(S1): E161–E178. https://doi.org/10.1002/joc.7530

UNEP (2025)a Emissions Gap Report 2025: Off Target — Continued collective inaction puts global temperature goals at risk. United Nations Environment Programme, Nairobi, Kenya. https://www.unep.org/resources/emissions-gap-report-2025

UNEP (2025)b Adaptation Gap Report 2025: Running on empty. UNEP, Nairobi, Kenya. https://www.unep.org/resources/adaptation-gap-report-2025

U.S. Environmental Protection Agency (2025) Extreme heat. https://www.epa.gov/climatechange-science/extreme-heat

Vautard R, Gobiet A, Sobolowski S, Kjellström E, Stegehuis A, Watkiss P, Mendlik T, Landgren O, Nikulin G, Teichmann C, Jacob D (2014) The European climate under a 2 °C global warming. Environmental Research Letters 9(3): 034006. https://doi.org/10.1088/1748-9326/9/3/034006

Von Storch H, Zwiers FW (2002) Statistical analysis in climate research. Cambridge University Press.

Wang L, Ranasinghe RWMRJB, Maskey S, van Gelder PHAJM, Vrijling JK (2016) Comparison of empirical statistical methods for downscaling daily climate projections from CMIP5 GCMs: a case study of the Huai River Basin, China. International Journal of Climatology 36(1): 145–164. https://doi.org/10.1002/joc.4334

Wartenburger R, Hirschi M, Donat MG, Greve P, Pitman AJ, Seneviratne SI (2017) Changes in regional climate extremes as a function of global mean temperature: an interactive plotting framework. Geoscientific Model Development 10(9): 3609–3634. https://doi.org/10.5194/gmd-10-3609-2017

World Meteorological Organization (2025) State of the global climate 2024. WMO Publication No. 1347, Geneva. https://wmo.int/publication-series/state-of-global-climate-2024

Zelinka M, Myers T, McCoy D, Po-Chedley S, Caldwell P, Ceppi P, Klein S, Taylor K (2020) Causes of higher climate sensitivity in CMIP6 models. Geophysical Research Letters 47. https://doi.org/10.1029/2019GL085782

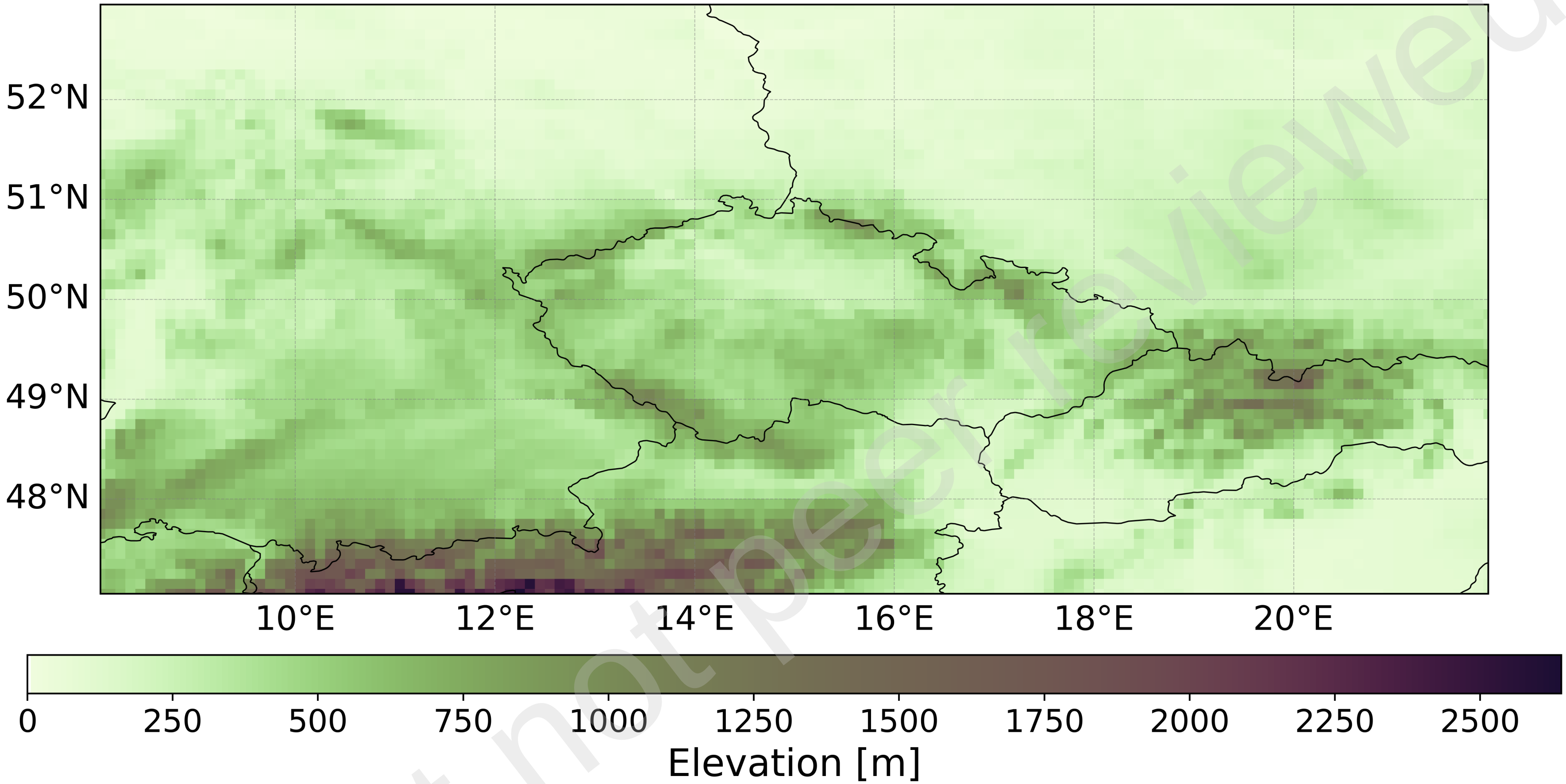

52°N
51°N
50°N
49°N
48°N
10°E
12°E
14°E
16°E
18°E
20°E
0
250
500
750
1000
1250
1500
1750
2000
2250
2500
Elevation [m]

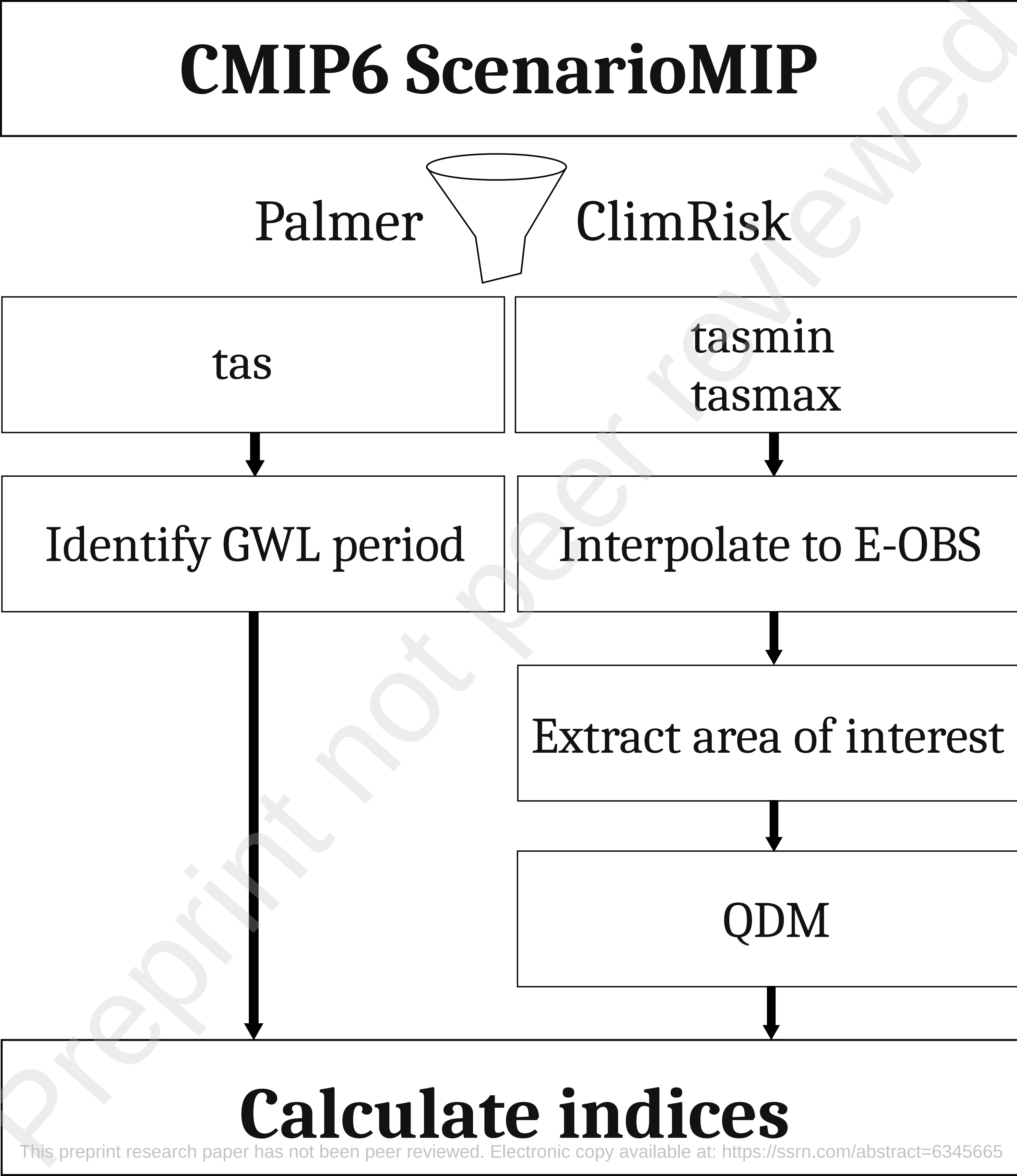
CMIP6 ScenarioMIP
Palmer
ClimRisk
tas
tasmin
tasmax
Identify GWL period
Interpolate to E-OBS
Extract area of interest
QDM
Calculate indices

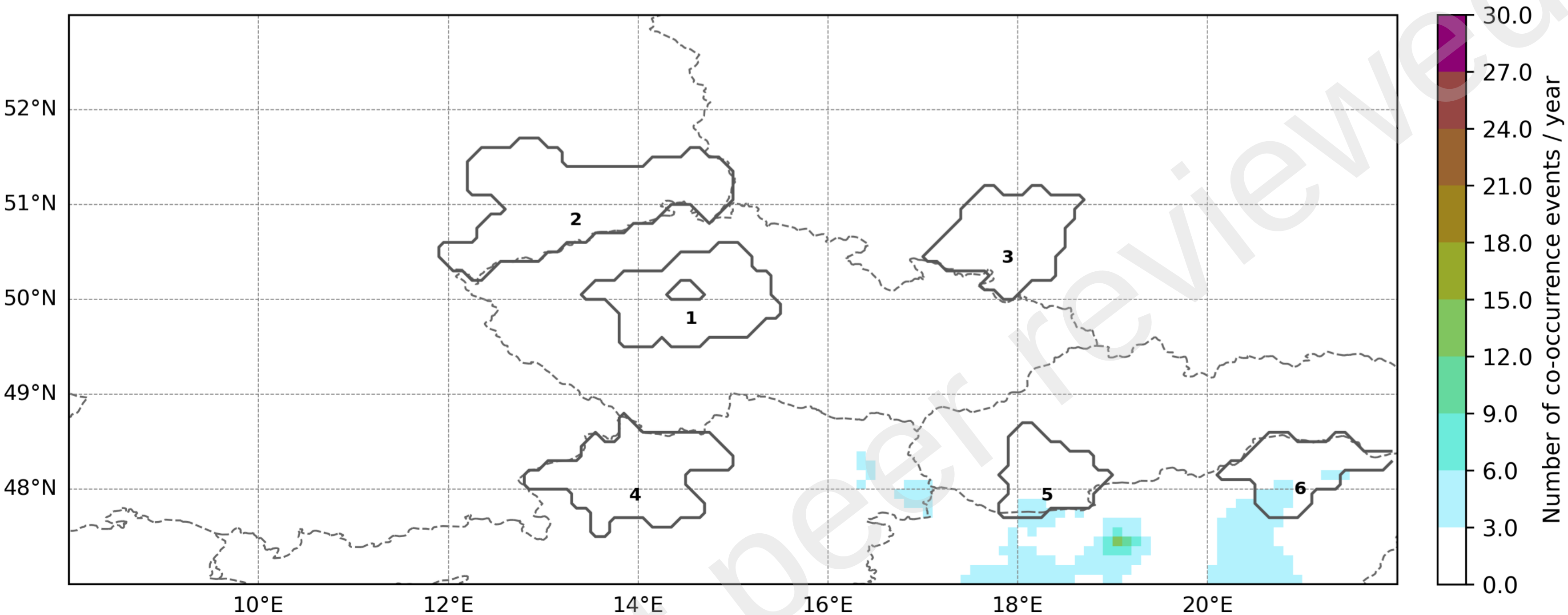

52°N
51°N
50°N
49°N
48°N
10°E
12°E
14°E
16°E
18°E
20°E
1
2
3
4
5
6
30.0
27.0
24.0
21.0
18.0
15.0
12.0
9.0
6.0
3.0
0.0
Number of co-occurrence events / year

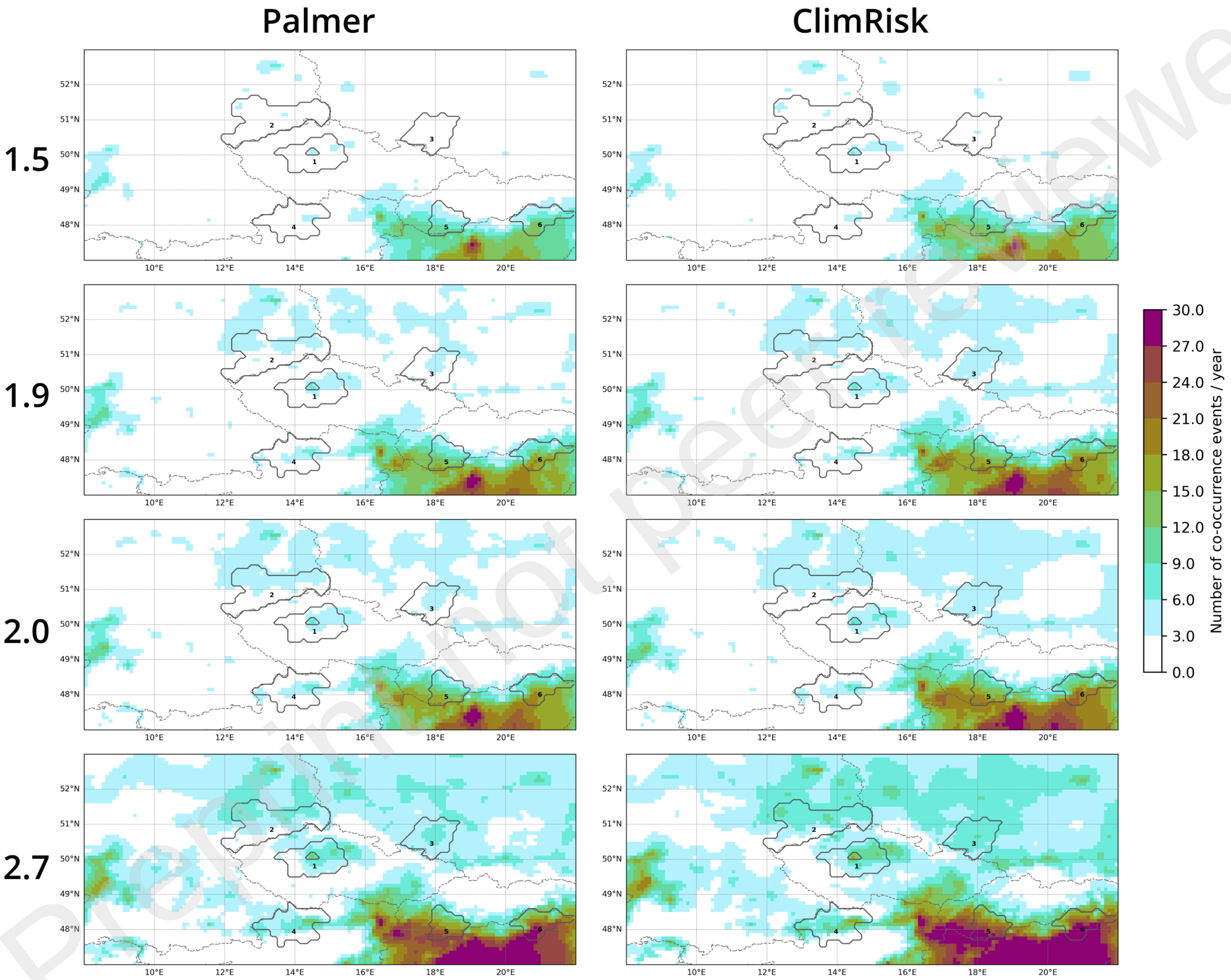

Palmer
ClimRisk
1.5
1.9
2.0
2.7
52°N
51°N
50°N
49°N
48°N
10°E
12°E
14°E
16°E
18°E
20°E
1
2
3
4
5
6
30.0
27.0
24.0
21.0
18.0
15.0
12.0
9.0
6.0
3.0
0.0
Number of co-occurrence events / year

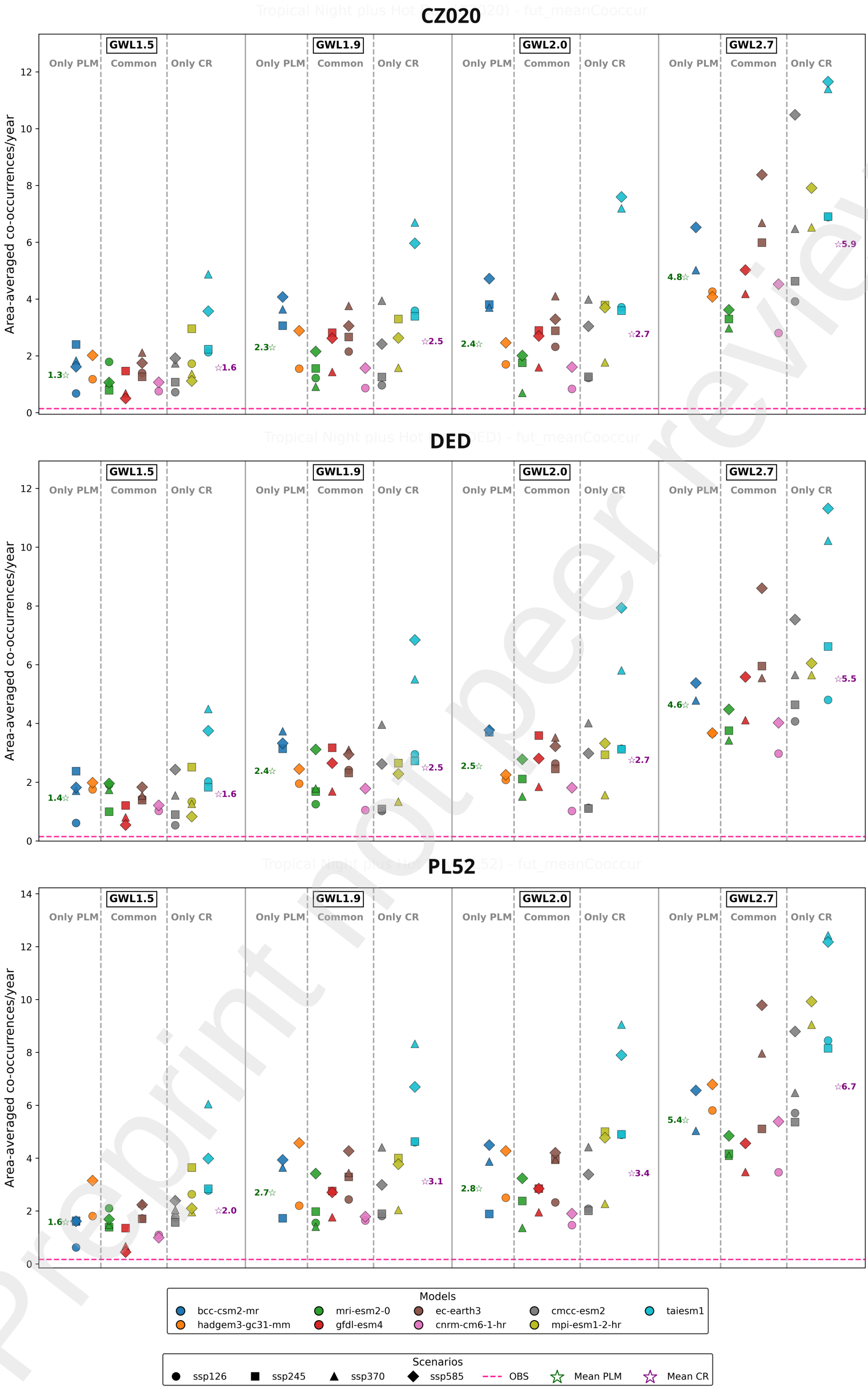
CZ020
DED
PL52
GWL1.5
GWL1.9
GWL2.0
GWL2.7
Only PLM
Common
Only CR
Area-averaged co-occurrences/year
1.3☆
☆1.6
2.3☆
☆2.5
2.4☆
☆2.7
4.8☆
☆5.9
1.4☆
☆1.6
2.4☆
☆2.5
2.5☆
☆2.7
4.6☆
☆5.5
1.6☆
☆2.0
2.7☆
☆3.1
2.8☆
☆3.4
5.4☆
☆6.7
Models
bcc-csm2-mr
hadgem3-gc31-mm
mri-esm2-0
gfdl-esm4
ec-earth3
cnrm-cm6-1-hr
cmcc-esm2
mpi-esm1-2-hr
taiesm1
Scenarios
ssp126
ssp245
ssp370
ssp585
OBS
Mean PLM
Mean CR

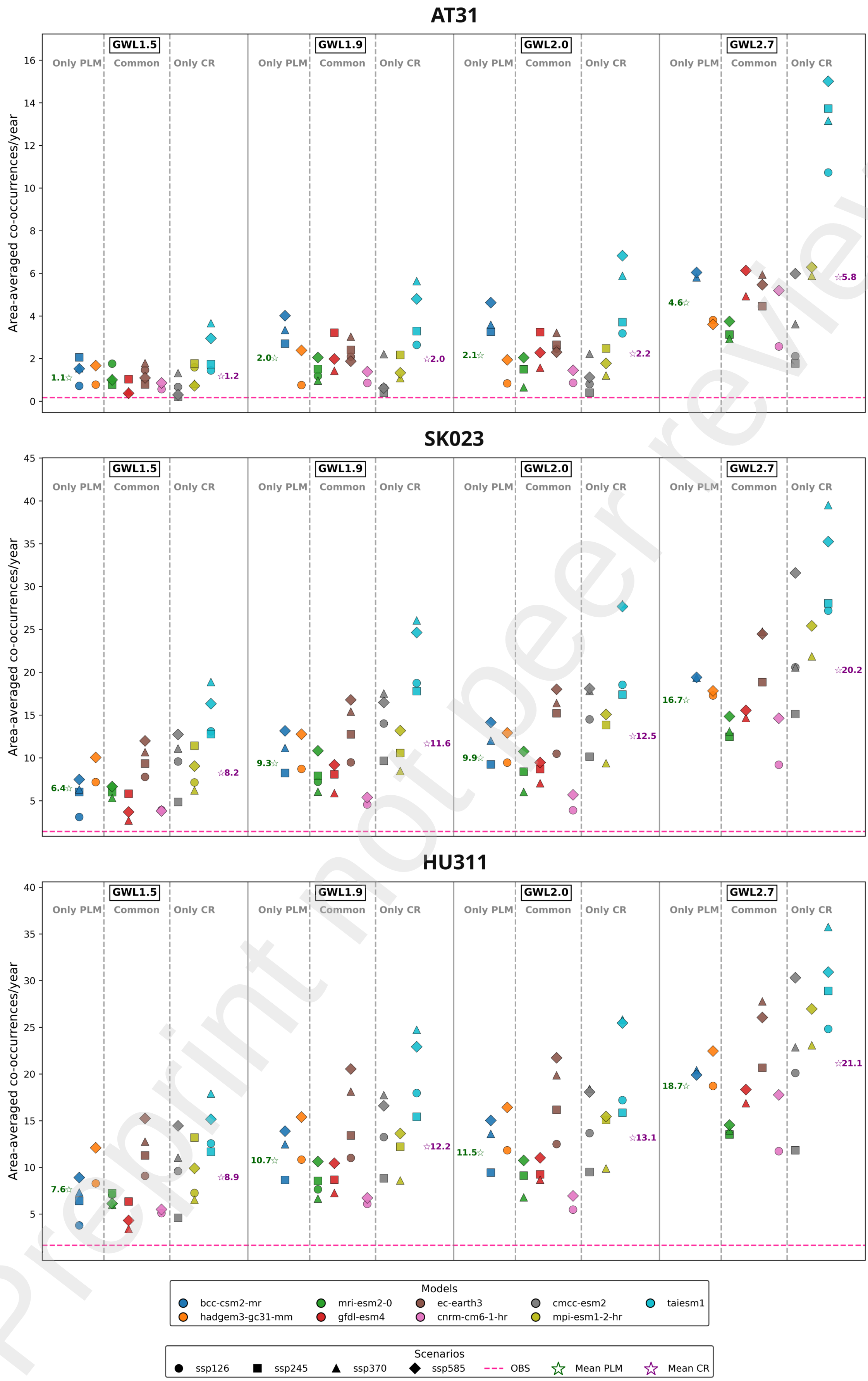

AT31
SK023
HU311
GWL1.5
GWL1.9
GWL2.0
GWL2.7
Only PLM
Common
Only CR
Area-averaged co-occurrences/year
Models
bcc-csm2-mr
hadgem3-gc31-mm
mri-esm2-0
gfdl-esm4
ec-earth3
cnrm-cm6-1-hr
cmcc-esm2
mpi-esm1-2-hr
taiesm1
Scenarios
ssp126
ssp245
ssp370
ssp585
OBS
Mean PLM
Mean CR